Nonlinear elastic load–displacement relation for spherical indentation on rubberlike materials

D.X. Liu
Department of Civil and Environmental Engineering, University of California, Irvine, California 92697-2175

Z.D. Zhang
Shenyang National Laboratory for Materials Science, Institute of Metal Research, Chinese Academy of Sciences, Shenyang 110016, China

L.Z. Sun[a)]
Department of Civil and Environmental Engineering, University of California, Irvine, California 92697-2175

(Received 14 April 2010; accepted 09 August 2010)

Because of the lack of universal contact models for nonlinear strain problems, indentation analysis on rubberlike materials is confined to small deformation in which Hertz's solution is applied. Recognizing that deep indentation may provide more material information, in this paper we propose a nonlinear elastic model for large spherical indentation of rubberlike materials based on the higher-order approximation of spherical function and Sneddon's solution. The effect of limiting network stretch is studied on the initial elastic modulus for lightly cross-linked rubbers. With the comparisons of the finite-element simulation and the experimental result, the proposed model is verified to predict the large indentation of rubberlike materials over the indentation depth of 0.8 times the indenter radius.

I. INTRODUCTION

Load–displacement curves of indentation include useful information of material properties, based on which the modulus and the hardness can be directly extracted as suggested by Oliver and Pharr.[1] An ISO standard was also released as a reference to guide indentation tests and analysis of metallic materials.[2] New areas for indentation application are rapidly emerging as recently published in the special issue of *Journal of Materials Research* in 2009 [Vol. 24(3)], focusing on indentation methodologies in advanced materials research.[3] However, indentation testing and analysis is less prevalent in the field of soft matter such as rubberlike materials. One of the primary reasons is that no existing universal contact-models of large strain are available. As a result, indentation of rubberlike materials is usually confined to small strain (shallow indentation) so that Hertz's solution is valid because its solution is only suitable for cases in which the ratio of the contact radius to the radius of the indenter is less than 0.1[4–6]; i.e., $a/R < 0.1$, where a is the contact radius and R is the radius of spherical indenter. It is noted that a/R is also referred to as the indentation strain.[7]

Depending on the extent of cross-linking, the extensibility in uniaxial extension of typical rubberlike materials is large and varies significantly.[8] Therefore, deeper indentation helps understand the rubberlike response. Some rubberlike materials are so soft that it is difficult to perform shallow indentation because of the low instrumentation compliance related to the load resolution.[9] To a certain degree, increasing indentation depth can overcome such difficulty. Research on large indentation of rubberlike materials makes much sense and is desirable. Nevertheless, the material and geometric nonlinearities frequently raise challenges to model the indentation of rubberlike materials with analytical attempts. Based on Hertz's linear solution and Mooney–Rivlin model, Lin and Horkay suggested a load–displacement equation proven valid in the testing of certain gels and soft tissues.[6,10,11] Further, Sabin and Kaloni found a second-order elastic solution for an incompressible material that predicts a stiffer response compared with Hertz's solution.[12] Giannakopoulos and Triantafyllou[13] also developed a model with a stiffer response than that predicted by Sabin and Kaloni. It is noted that all these solutions have a common mainstay that the shape function of the spherical indenter is approximated as $r^2/2R$, the first-order approximation of the Taylor expansion with the notations of r (radius coordinate) and R (indenter radius) as shown in Fig. 1, which makes the indentation strain under 30%.

With indentation depth increasing, the first-order approximation of spherical shape may not be appropriate.

[a)]Address all correspondence to this author.
e-mail: lsun@uci.edu
DOI: 10.1557/JMR.2010.0285

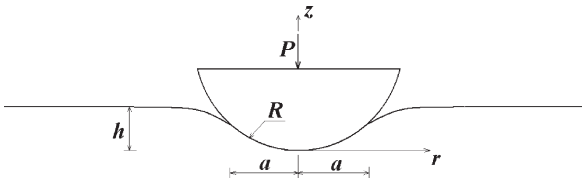

FIG. 1. Geometric schematic diagram of the spherical indentation.

In this article, a nonlinear elastic model is proposed for large spherical indentation of rubberlike materials based on a higher-order approximation of spherical function. The model takes into account the effect of the limiting network stretch on the initial elastic modulus. With the comparisons of Hertz's model, Giannakopoulos and Triantafyllou's model[13] (G&T model), the finite element simulation, and the experimental indentation data, the proposed model is verified to predict the large indentation of rubberlike materials over the indentation depth of 0.8 times the indenter radius; i.e., indentation strain of 80%.

II. LOAD–DISPLACEMENT RELATION FOR LARGER INDENTATION ON RUBBERLIKE MATERIALS

When a load P is applied to the punch, it is displaced into the half space of the rubberlike material by an amount h, producing a circle of contact at the surface with radius a, as shown in Fig. 1. Previous investigations of related work take advantage of the first-order approximation of the Taylor expansion of spherical functions. However, such approximation normally results in a deviation from realistic cases on the condition of deep indents ($a/R > 30\%$ or $h/R > 10\%$).

To better predict the large indentation on rubberlike materials, the description of the indenter shape function f should be dealt with a higher-order approximation of the spherical function; i.e., the first two terms of the Taylor expansion are kept:

$$f(r) = (R - \sqrt{R^2 - r^2}) \approx \frac{r^2}{2R} + \frac{r^4}{8R^3} \quad . \tag{1}$$

Furthermore, the deduction of the load displacement relation is conducted by recourse to Sneddon's work. Using the Hankel transform, Sneddon[14] derived the expressions for the load P and the displacement h for a punch of arbitrary profile,

$$h = \int_0^1 \frac{f'(x)}{\sqrt{1 - x^2}} dx \quad , \tag{2}$$

$$P = \frac{4\mu a}{1 - \nu} \int_0^1 \frac{x^2 f'(x)}{\sqrt{1 - x^2}} dx \quad , \tag{3}$$

where x is a dimensionless variable defined as $x = r/a$ such that in the region of contact, $0 < x < 1$, $f'(x)$ is the derivative of the spherical function with respect to x, μ is the shear modulus, and ν is the Poisson ratio. The detailed derivation of Eqs. (2) and (3) can be found in Sneddon's work.[14] For rubberlike materials with the Poisson ratio assumed to be 0.5 for simplicity, the explicit formula of the displacement and load can be derived by substituting Eq. (1) into Eqs. (2) and (3):

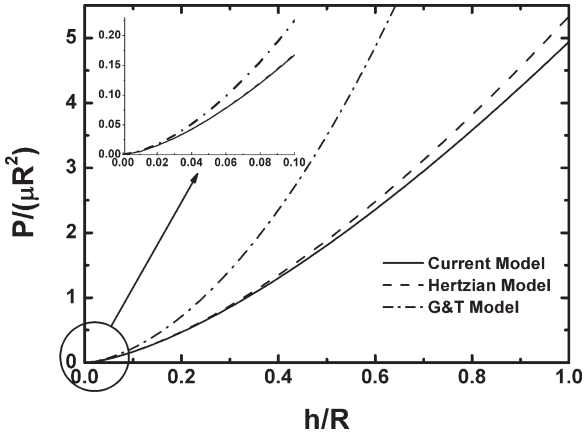

FIG. 2. Comparisons among Hertz's model, G&T model, and Eq. (5) for the relationship of spherical punch load P and the displacement h.

$$h = \frac{a^2}{R} + \frac{a^4}{3R^3} \quad , \tag{4}$$

and

$$P = \frac{16}{9} E a^3 \left(\frac{1}{R} + \frac{2a^2}{5R^3} \right) \quad , \tag{5}$$

where E is the initial elastic modulus. The comparisons of punch load–displacement relationship among Hertz's model, G&T model, and Eq. (5) are shown in Fig. 2. It is noted that Eq. (5) presents a softer load as compared with Hertz's and G&T's models, which stems from Eq. (4) that the displacement approaches a more realistic scenario of geometric shape when the indentation depth increases. This statement is further supported by finite element results in the next section (Sec. III) shown in Figs. 3 to 5. It is expected that Eqs. (4) and (5) can provide a reasonable fit with indentation strain up to 80% for Mooney–Rivlin materials and Neo–Hookean materials.

As learned from statistical mechanics, the elasticity of cross-linked rubber materials models the chain between chemical cross-links as a number N of rigid links of equal length l. The initial chain length is then derived as $\sqrt{N}l$, and the limiting network stretch λ_L (the maximum value of the stretch λ) is further obtained as $\lambda_L = \sqrt{N}$.[8,15] As for rubbers, the variation of the initial elastic modulus with stretch relies on the limiting network stretch λ_L. When λ_L is large, the initial elastic modulus of the rubber

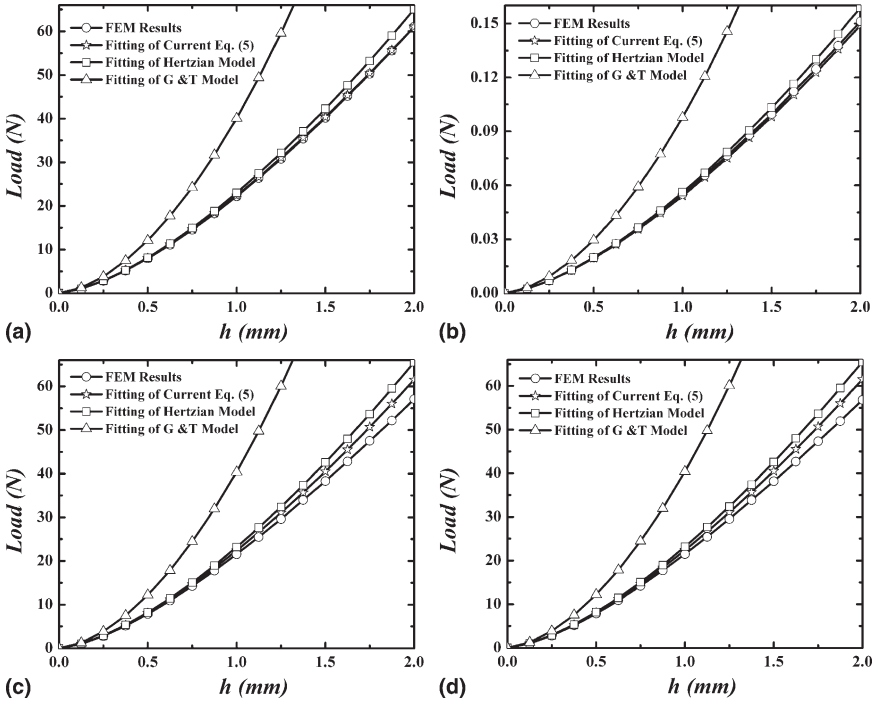

FIG. 3. FEM simulation of Mooney-Rivlin materials and the fitting results of different models with the indenter radius of 2.5 mm: (a) $c_1 = c_2 = 0.6871$ MPa; (b) $c_1 = 1.33 \times 10^{-3}$ MPa and $c_2 = 2 \times 10^{-3}$ MPa; (c) $c_1 = 1.34$ MPa and $c_2 = 0.0342$ MPa; (d) $c_1 = 1.3742$ MPa and $c_2 = 0$.

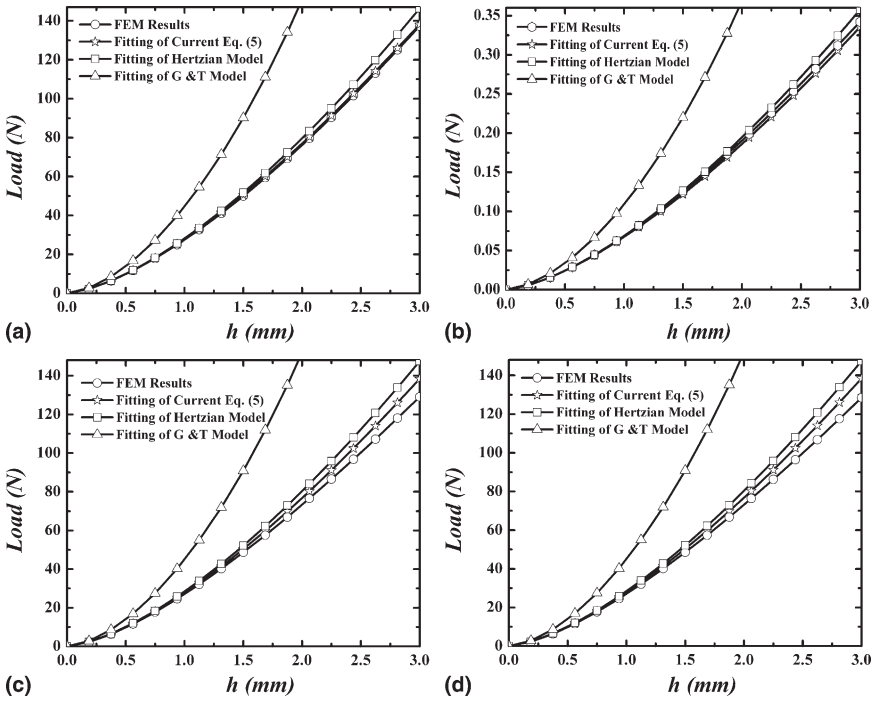

FIG. 4. FEM simulation of Mooney–Rivlin materials and the fitting results of different models with the indenter radius of 3.75 mm: (a) $c_1 = c_2 = 0.6871$ MPa; (b) $c_1 = 1.33 \times 10^{-3}$ MPa and $c_2 = 2 \times 10^{-3}$ MPa; (c) $c_1 = 1.34$ MPa and $c_2 = 0.0342$ MPa; (d) $c_1 = 1.3742$ MPa and $c_2 = 0$.

exhibits an ignorable fluctuation. However, as the limiting network stretch decreases, the initial elastic modulus increases rapidly, which can be justified in the eight-chain material model.[15,16] Initial elastic moduli can be calculated as the slope of the stress–stretch curve at the stretch-free position.

As an example, for the eight-chain model[15] which incorporates λ_L as a variable, the initial elastic modulus reads

$$E^* = [\partial\Psi/\partial\lambda + \lambda(\partial^2\Psi/\partial\lambda^2)]|_{\lambda=1} \quad , \qquad (6)$$

with the strain energy density obtained from the eight-chain model

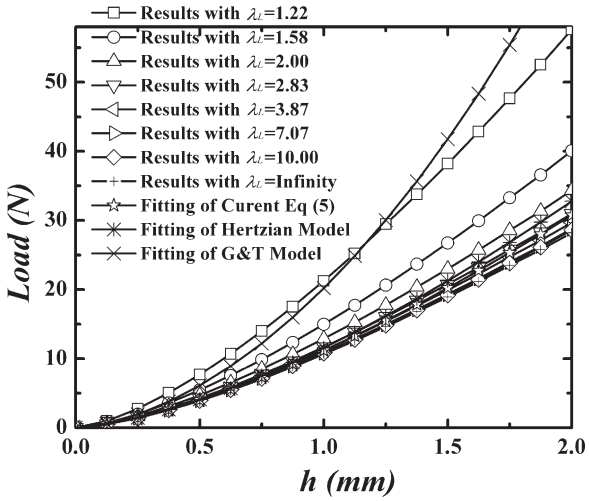

FIG. 5. FEM simulation of Arruda–Boyce materials and the fitting results with different models.

$$\Psi = \mu\left[\frac{1}{2}(I_1-3)+\frac{1}{20\lambda_L^2}(I_1^2-9)+\frac{11}{1{,}050\lambda_L^4}(I_1^3-27)+\frac{19}{7{,}000\lambda_L^6}(I_1^4-81)+\frac{519}{672{,}750\lambda_L^8}(I_1^5-243)\right]+\ldots. \quad (7)$$

When the limiting network stretch is large, the elastic modulus of the eight-chain model is similar to the linear elastic model, which is three times that of the shear modulus. However, the initial elastic modulus increases rapidly as the limiting network stretch is small, underlining the different physical basis from linear elastic model. The difference may be caused by a greater degree of strain hardening to lightly cross-linked rubberlike materials shown in the eight-chain model.

For the Mooney–Rivlin model,[11] the initial elastic modulus can be calculated as

$$E^* = \frac{\partial^2 \Psi}{\partial \lambda^2}|_{\lambda=1} \quad , \quad (8)$$

with the strain energy density

$$\Psi = c_1(I_1-3)+c_2(I_2-3) \quad , \quad (9)$$

where I_1 is the first stretch invariant, I_2 is the second stretch invariant, and c_1 and c_2 are material constants. When c_2 is equal to zero, it goes to Neo-Hookean model, which is equivalent to the eight-chain model of an infinite λ_L.

For lightly cross-linked rubbers, the load of indentation in Eq. (5) can be underestimated for materials of low limiting network stretches without the consideration of the effect of λ_L on the initial modulus (more details in Sec. III). Therefore, Eq. (5) can be modified further for accommodating lightly cross-linked rubbers as:

$$P = \frac{16}{9}E^* a^3\left(\frac{1}{R}+\frac{2a^2}{5R^3}\right) \quad . \quad (10)$$

It is noted that Eq. (10) can be reduced to Eq. (5) for the Mooney–Rivlin model or the Neo-Hookean model since E^* is 3μ for the two models. However, Eq. (4) is independent of material properties and therefore does not call for any changes that account for the modulus increasing. Therefore, the load–displacement relations proposed in Eqs. (4) and (10) can be used to predict the indention of rubberlike materials. In next section, finite element method (FEM) is used to simulate the indentation process covering a wide range of limiting network stretches.

III. FEM VERIFICATION AND EXPERIMENTAL VALIDATION

FEM simulations on Mooney–Rivlin materials and Arruda–Boyce materials with MSC.MARC are performed to verify the current model, Eqs. (4), (5), and (10). Material constants of the Mooney–Rivlin material description follow those appearing in literature[13,17]: (a) $c_1 = c_2 = 0.6871$ MPa, (b) $c_1 = 1.33 \times 10^{-3}$ MPa and $c_2 = 2 \times 10^{-3}$ MPa, (c) $c_1 = 1.34$ MPa and $c_2 = 0.0342$ MPa, (d) $c_1 = 1.3742$ MPa and $c_2 = 0$. The Mooney–Rivlin material just with one constant ($c_2 = 0$) is compatible with the Neo-Hookean material.[10] Material constants of the Arruda–Boyce material in current simulation are described with the common initial shear modulus, 1.3742 MPa, and different limiting network stretch λ_L, 1.22, 1.58, 2.00, 2.83, 3.87, 7.07, 10.00, and infinity. The Arruda–Boyce material with an infinite λ_L is also compatible with the Neo-Hookean material.

The indentation simulation is modeled as an axisymmetric problem consisted of 63,531 elements and 64,029 nodes. Near the contact region, greater and finer numbers of elements are meshed so that enough elements can be involved in the contact. The ball indenter is assumed rigid and has the radius of either 2.5 or 3.75 mm. The outer dimensions of the model are at least 30 times the maximum contact depth and the maximum contact radius. The contact interface is assumed frictionless. When simulated, the indenter is penetrated into materials with a constant speed until the maximum depth reaches to 0.8 R.

The simulation results of Mooney–Rivlin materials and the fitted results by different models are shown in Figs. 3 and 4, from which it can be shown that the current model presents an excellent prediction through h/R of 80% for softer materials, and then the maximum indentation strain a/R is almost as high as 81%. The load error from current model Eq. (5) is only 7% when h/R is 80%. As a comparison, the Hertz model works well through h/R of 35%. The G&T model overestimate the load values

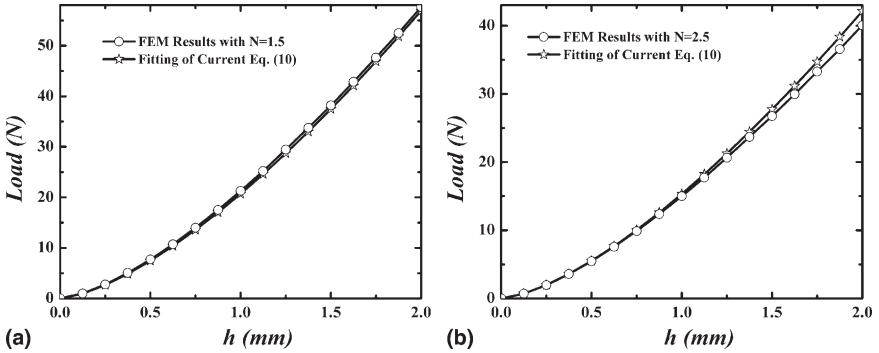

FIG. 6. The prediction of Eq. (10) with consideration of the effect of the limiting network stretch on the initial elastic modulus.

even when h/R is under 10% for Mooney–Rivlin and Neo-Hookean materials.

Figure 5 illustrates the simulation results of indentation of Arruda–Boyce materials in which decreased limiting network stretch λ_L results in increased load at same displacement as a similar finding was reported in Ref. 16. The radius of indenter R is 2.5 mm. It is noted that Eq. (5) underestimates the load of the indentation of materials with the smaller limiting network stretch that leads to the rapid increase of the initial elastic modulus as analyzed previously. It is also not expected that, even under h/R of 10%, the G&T model makes better predictions than Eq. (5) does as shown in Fig. 5. As a result, Eq. (10) with consideration of the effect of the limiting network stretch on the modulus should further be tried as shown in Fig. 6, which demonstrates that the prediction of Eq. (10) perfectly agrees with the results of FEM simulation.

Comparisons are further conducted between the proposed model and experiment. Tan et al.[5] experimentally studied the indentation of ethylene-propylene-diene monomer (EPDM) materials. Experimental data of EPDM samples after 47 week exposure at 60 °C with the applied pressure of 0.77 MPa is selected that holds the elastic modulus of 8.67 MPa. The limiting network stretch of the EPDM sample is then extracted as $\lambda_L = 1.90$ by fitting eight-chain model. Figure 7 illustrates the comparison between the predicted results [Eq. (5) and Eq. (10)] and the experimental data of EPDM. It can be seen that the proposed model [Eq. (10)] agrees well with the experimental data. Figure 8 shows another comparison between the model prediction and the experimental data by Giannakopoulos and Triantafyllou[13] for an incompressible rubber material with indentation radius $R = 4.75$ mm. It is demonstrated that the prediction of Eq. (10) agrees better with the experimental results than the prediction of Eq. (5).

It is noted that the current model takes advantage of Sneddon's solution,[14] which is a general relationship among the load, displacement, and contact area for a rigid, axisymmetric punch contacting on an elastic half

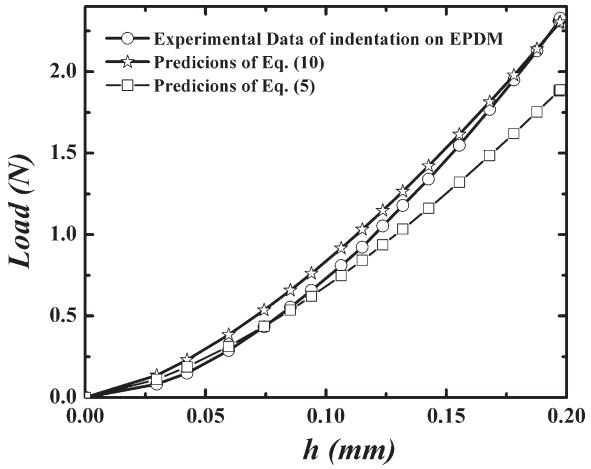

FIG. 7. Comparisons between the current model and the experimental data of indentation on EPDM materials.

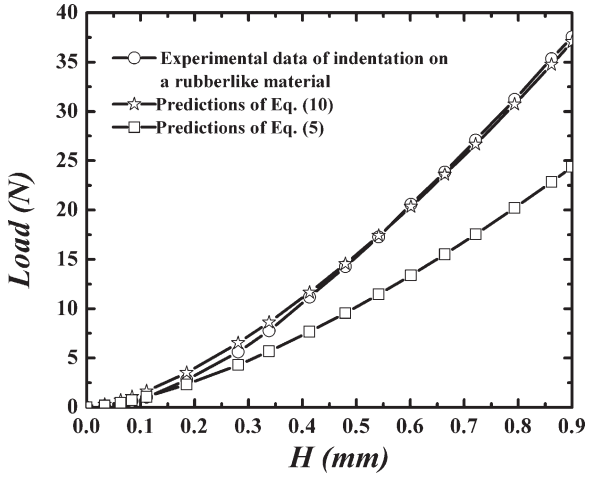

FIG. 8. Comparisons between the current model and the experimental data of indentation on rubberlike materials.

space. Such relationship is useful for the determination of mechanical properties using indentation techniques originally proposed by Pharr et al.[18] While applicable for any smooth function of $f(x)$, Sneddon's analysis is based on infinitesimal-deformation theory with the

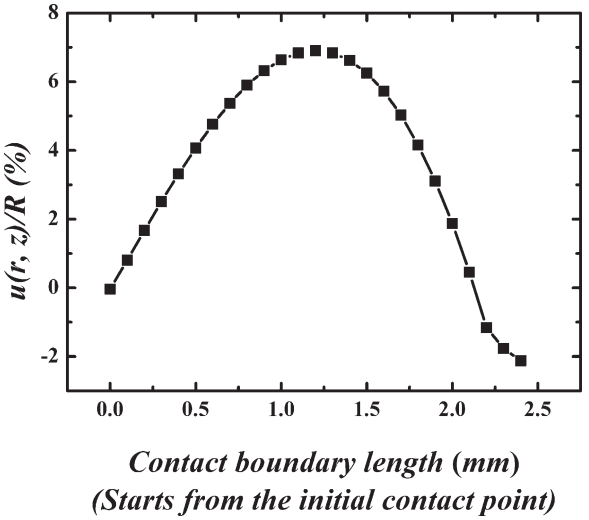

FIG. 9. Dependence of horizontal displacement $u(r,z)/R$ on the punch contact boundary.

horizontal displacement under the indenter assumed zero. It is acknowledged that such small deformation theory may not deliver accurate estimation for nonlinear deformation problems in general. For the specific spherical-indentation case, the fully nonlinear finite element simulation is conducted to compute the horizontal displacement $u(r, z)$ of Arruda–Boyce material. Figure 9 shows that, as maximum value of the stretch $\lambda_L = 10$, the ratio of $u(r, z)$ over indenter radius R is quite small (less than 7%) even in the case of a/R up to 80%, demonstrating that the current model has the capability of estimating nonlinear elastic responses under deep indentation. Despite of the support of nonlinear numerical simulation, more work on full geometric nonlinearity should be needed in future work.

IV. CONCLUSIONS

A nonlinear elastic model is proposed for large spherical indentation of rubberlike materials based on the two-term approximation of spherical function and the Sneddon solution. The model is specially designed to account for the effect of the limiting network stretch on the initial elastic modulus. The capability of the proposed model is verified by comparison with the finite element simulations on the Mooney–Rivlin, Neo-Hookean, and Arruda–Boyce materials. Furthermore, the model is experimentally validated to be accurate with the large indentation responses of cross-linked rubbers. It is expected that the proposed model is feasible for materials exhibiting rubber elasticity without the limitation of shallow indentation (linear scope). The indentation depth can be extended to 0.8 times the indenter radius.

ACKNOWLEDGMENTS

The authors would like to thank the anonymous reviewers for their constructive comments and suggestion. This work is sponsored in part by NSF with Grant No. CMMI-0800417 and in part by the CAS/SAFEA International Partnership Program for Creative Research Teams, whose supports are gratefully acknowledged.

REFERENCES

1. W.C. Oliver and G.M. Pharr: An improved technique for determining hardness and elastic modulus using load and displacement sensing indentation experiments. *J. Mater. Res.* **7,** 1564 (1992).
2. ISO 14577: *Metallic Materials—Instrumented Indentation Test for Hardness and Materials Parameters* (International Organization for Standardization, Geneva, Switzerland, 2002).
3. G.M. Pharr, Y-T. Cheng, I.M. Hutchings, M. Sakai, N.R. Moody, G. Sundararajan, and M.V. Swain: Focus issue on indentation methods in advanced materials research. *J. Mater. Res.* **24**(3), 579 (2009).
4. K.L. Johnson: *Contact Mechanics* (Cambridge University Press, Cambridge, UK, 1985).
5. J. Tan, Y.J. Chao, J.W. Van Zee, X. Li, X. Wang, and M. Yang: Assessment of mechanical properties of fluoroelastomer and EPDM in a simulated PEM fuel cell environment by micro-indentation test. *Mater. Sci. Eng., A* **496,** 464 (2008).
6. D.C. Lin, E.K. Dimitriadis, and F. Horkay: Elasticity of rubber-like materials measured by AFM nanoindentation. *eXPRESS Polym. Lett.* **9,** 576 (2007).
7. A.C. Fisher-Cripps: *Nanoindentation* (Springer Press, New York, 2002).
8. I.M. Ward and J. Sweeney: *An Introduction to the Mechanical Properties of Solid Polymers*, 2nd ed. (Wiley Press, Chichester, UK, 2004), pp. 32, 36.
9. M.R. VanLandingham, J.S. Villarrubia, W.F. Guthrie, and G.F. Meyers: Nanoindentation of polymer: An overview. *Macromol. Symp.* **167,** 167 (2001).
10. D.C. Lin and F. Horkay: Nanomechanics of polymer gels and biological tissues: A critical review of analytical approaches in the Hertzian regime and beyond. *Soft Mater.* **4,** 669 (2008).
11. R.S. Rivlin: Large elastic deformations of isotropic materials: IV. Future developments of the general theory. *Philos. Trans. R. Soc. London, Ser. A* **241,** 379 (1948).
12. G.C.W. Sabin and P.N. Kaloni: Contact problem of a rigid indenter with notational friction in second order elasticity. *Int. J. Eng. Sci.* **27,** 203 (1989).
13. A.E. Giannakopoulos and A. Triantafyllou: Spherical indentation of incompressible rubber-like materials. *J. Mech. Phys. Solids* **55,** 1196 (2007).
14. I.N. Sneddon: The relation between load and penetration in the axisymmetric Boussinesq problem for a punch of arbitrary profile. *Int. J. Eng. Sci.* **3,** 47 (1965).
15. E.M. Arruda and M.C. Boyce: A three-dimensional constitutive model for the large stretch behavior of rubber elastic materials. *J. Mech. Phys. Solids* **41,** 389 (1993).
16. I. Kang, D. Panneerselvam, V.P. Panoskaltsis, S.J. Eppell, and R.E. Marchant: Changes in the hyperelastic properties of endothelial cells induced by tumor necrosis factor-α. *Biophys. J.* **94,** 3273 (2008).
17. H. Yin, L.Z. Sun, G. Wang, T. Yamada, J. Wang, and M. Vannier: ImageParser: A tool for finite element generation from three-dimensional medical images. *Biomed. Eng. Online* **3,** 31 (2004).
18. G.M. Pharr, W.C. Oliver, and F.R. Brotzen: On the generality of the relationship among contact stiffness, contact area, and elastic modulus during indentation. *J. Mater. Res.* **7,** 613 (1992).